1992

Analysis of Screw Compressor Performance Based on Indicator Diagrams

K. Miyoshi
Kobe Steel Ltd.; Japan

ANALYSIS OF SCREW COMPRESSOR PERFORMANCE BASED ON INDICATOR DIAGRAMS

Kiyotada Miyoshi
Senior Researcher, Technology Development Center,
Kobe Steel Ltd.
Kobe, Japan

ABSTRACT

By means of a small pressure sensor built into the tooth root on the discharge side of the female rotor, the pressure change in the groove can be measured from the midpoint of the suction stroke to the completion of the discharge. Indicator diagrams were collected for a single stage cycle and the indicated horsepower was calculated. In this manner, we could determine the gas compression conditions inside the groove and thus the data could be analyzed for furthering the studies on high-efficiency profiles.

1. Introduction

Screw compressor performance has in the past been experimentally sought from operating data by varying the rotation speed and pressure ratio to match each rotor outer diameter and built-in pressure ratio. However, as it was impossible to grasp the pressure rise phenomenon inside the rotor groove, this method was not useful in studying tooth profile or improvements in the discharge and suction ports. As for changing the rotor tooth profile, the high price of the cutter blade for processing the rotor profile and the necessary jigs has to date been an impediment to realizing trial production and test runs in order to make performance comparisons.

The author has been successful in grasping the loss of gas due to leakage between rotor grooves and the excessive compression phenomenon at the discharge port by computing pressure changes inside the rotor groove during compressor operation. The following is a report on the results of my study.

Nomenclature

Cv: Constant volume specific heat, J (kg・K)
D: Rotor diameter, mm
k: Specific heat ratio
L: Compression work, W
Lth: Theoretical adiabatic compression power, W
Lpv: Indicated power, W
l: Rotor length, mm
M: Gas weight, kg
Mi: Groove gas leak-in weight, kg
Mo: Groove gas leak-out weight, kg
mth: Theoretical suction gas weight flow rate, kg/s
mac: Actual suction gas weight flow rate, kg/s
N: Male rotor rotation, rpm
P: Gas pressure, Pa
Ps: Suction gas pressure, Pa
Pd: Discharge gas pressure, Pa
R: Gas constant, J/(kg・K)
T: Gas temperature, °K
t: Time, sec.
V: Gas volume, m^3
Vo: Theoretical stroke volume, m^3
Vi: Built-in volume ratio
η ad: Adiabatic efficiency
η v: Volumetric efficiency
π i: Built-in pressure ratio, $=V_i^k$
θ : Male rotor rotation angle, deg.

2. Theoretical Calculation of Performance

In order to analyze screw compressor performance, changes in the seal area and volume of the rotor groove space were computed for every rotation angle of the male rotor, based on which increases in gas pressure and temperature following the rotor rotation are simulated in order to construct an indicator diagram [1] ~ [2]. Fig. 1 shows rotor groove conditions during compression.

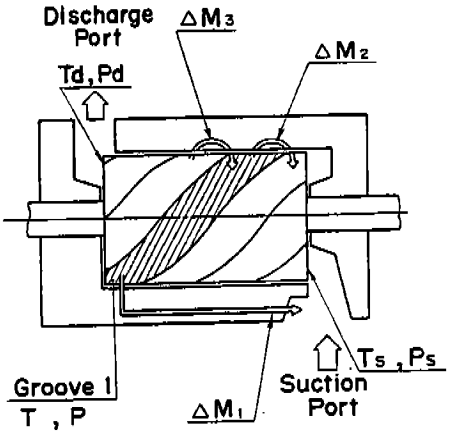

Fig. 1 Cross-section of screw compressor

For the computation, the following suppositions were used.

(1) Changes in gas condition or volume in the groove are stable;
(2) Gas passing through the seal area and discharge port is considered adiabatic change;
(3) Gas cooling effect by rotor or casing is not considered;
(4) Gas velocity due to rotor rotation is not considered. The change in gas weight in Groove 1 can be expressed by:

$$\left.\begin{aligned} dM_1 &= \Delta M_3 \\ dM_0 &= \Delta M_1 - \Delta M_2 \end{aligned}\right\} \quad \cdots\cdots (1)$$

$$\frac{dM}{dt} = \frac{dM_1}{dt} - \frac{dM_0}{dt} \quad (2)$$

The energy equation is:

$$\frac{dL}{dt} = \frac{dM_0}{dt} kC_1 T_0 - \frac{dM_1}{dt} kC_1 T + MC_1 \frac{dT}{dt} - C_1 T \frac{dM}{dt} \quad \cdots\cdots (3)$$

The compression work is:

$$\frac{dL}{dt} = -P \frac{dV}{dT} \quad \cdots\cdots (4)$$

From the equation of status:

$$\frac{dp}{P} = \frac{dM}{M} - \frac{dT}{T} - \frac{dV}{V} \quad \cdots\cdots (5)$$

By computing equations (1) to (5), changes in pressure and temperature inside the groove can be simulated.

3. Method of collecting indicator diagrams

As the screw compressor is so structured that the groove volume is reduced as the male and female rotors are engaged, gas is compressed towards the discharge side. Therefore if a small piezoelectric pressure sensor is built into the bottom of the discharge side female root, changes in pressure inside the groove from the midpoint of suction stroke to the completion of suction, and from the start of compression to the completion of discharge, can be measured.

Table 1 shows the main rotor specifications and Fig. 2 is a flow diagram of the measurement of indicator pressure.

As can be seen in the figure, the cord of the compact pressure sensor passes through the through hole at the center of the rotor and is connected to the slip ring by a Teflon coupling. Signals are sent to the signal analyzer, mounted outside, via the slip ring. The rotary-side flange of the slip ring has a notch in which a displacement gauge is externally mounted in order to determine the rotor suction angle/position.

Table 1 Main specifications of rotor

Combination of lobes number		
	Male	4
	Female	6
Rotor diameter	mm	100.0
Rotor length	mm	165.0
Wrap angle (male rotor)	deg	300.0
Built-in volume ratio		2.5

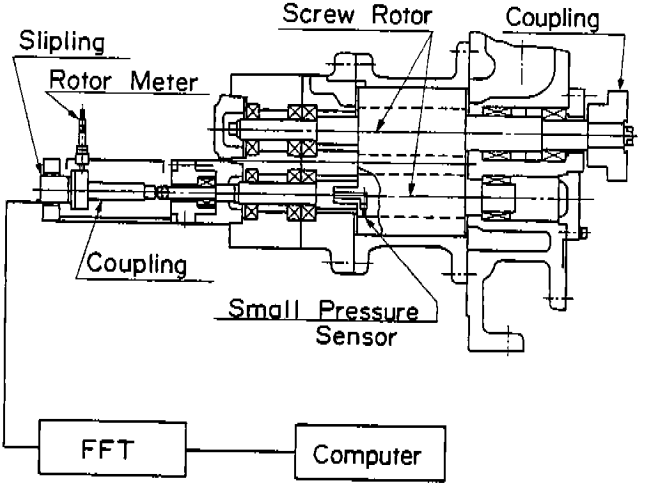

Fig. 2 Pressure sensor mounting diagram

The signal analyzer picks up the displacement gauge rotation signal and the pressure sensor signal at the same time: the sampling speed and the pressure range are changed over to match changes in the pressure ratio and rotation speed during the test so that highly precise data can be obtained.

For this test, measurements were made at the conditions of: rotor outer diameter=100ϕ, built-in volume ratio=Vi2.5, gas=R-22.

Fig. 3 shows the data so gathered correlated with the male rotor rotation angle θ on the abscissa and the change in pressure ratio P/Ps on the ordinate.

In this figure, the peak value appearing at the pitch of 540° is the signal per rotation of the female rotor. The 0 ° rotation angle is the point at which compression starts, and a sudden pressure drop is seen at the point at which discharge ends in the vicinity of 390 °.

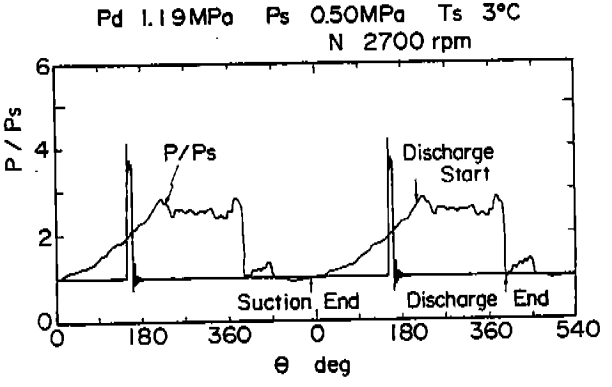

Fig. 3 Pressure change and rotor rotation angle

4. Indicator diagram and compressor efficiency

The screw compressor's built-in volume ratio Vi is designed to be 2.5. Hence it is so structured that the discharge port is opened when the stroke volume drops to about 40%. Unlike a reciprocal compressor, the screw compressor has no discharge valve or suction valve, and so the suction port can be made larger to match suction stroke, and the pressure of the suction port can be used as suction pressure.

The pressure inside the rotor groove continues rising; but, at the start of discharge, the flow area of gas at the time of port opening becomes extremely small.

Fig. 4 is a comparison of the actual and simulated indicator diagrams at male rotor rotation speeds of 3550 rpm and 2700 rpm. In Fig. 4, line a b represents suction stroke, line b-c is compression stroke, line c-d is discharge stroke, and line b-c'-d' represents result of computation. In that figure, the area within the line a b-c d-a is the actual indicated horsepower Lpv; if the theoretical adiabatic compression power at theoretical suction gas weight flow rate mth is Lth, the volumetric efficiency ηv can be expressed by:

$$\eta v = \frac{mac}{mth} \quad \cdots \quad (6)$$

The adiabatic efficiency ηad is:

$$\eta ad = \frac{Lth}{Lpv} \times \eta v \quad \cdots \quad (7)$$

By comparing the results of equation (6) and (7) with b-c-d and b-c'-d' in the P-V curve, that part where horsepower loss is generated can be found, making it possible to determine which points to improve in rotor profile and port shape in relation to performance.

By comparing the theoretical indicator diagram with the measured diagram in Fig. 4, it can be seen that the gas pressure is high shortly after compression starts, but it drops shortly before discharge. This is thought to be due to the fact that the seal between the rotors at the suction side suffers less gas leakage due to the presence of the oil film, but on the discharge side the oil film is broken by the high differential pressure, resulting in greater gas leakage.

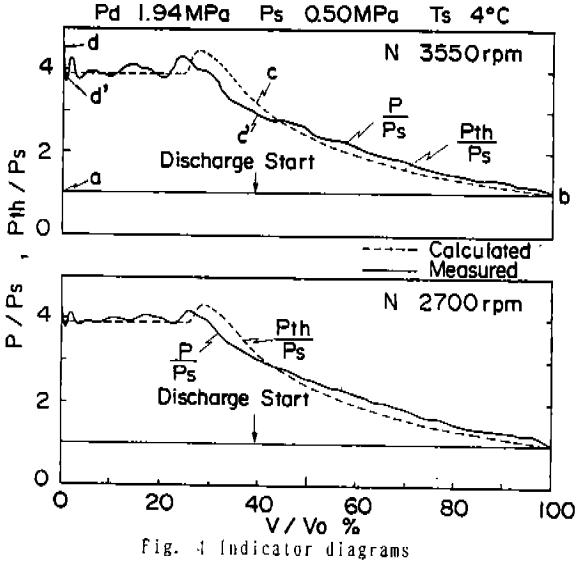

Fig. 4 Indicator diagrams

Fig. 5 and Fig. 6 are indicator diagrams when the pressure ratio is varied while suction pressure is kept constant. These figures show the result of making the pressure ratio greater than the design value of 3.0. In addition, suction pressure Ps 0.35 MPa data have also been gathered in order to study the effect at a high pressure ratio. From these figures, it can be seen that the pressure during the compression stage is affected greatly by the discharge pressure even if the built-in pressure ratio is kept constant.

Therefore, it may be assumed that the leakage of gas is great from the rotor end seal and the tip seal at the discharge side. On the other hand, as the discharge port area is proportional to the rotation angle at the start of discharge, the pressure inside the groove does not change abruptly shortly after the port is opened even at a pressure ratio other than the design ratio. Thus the pressure ratio can be within a broad range.

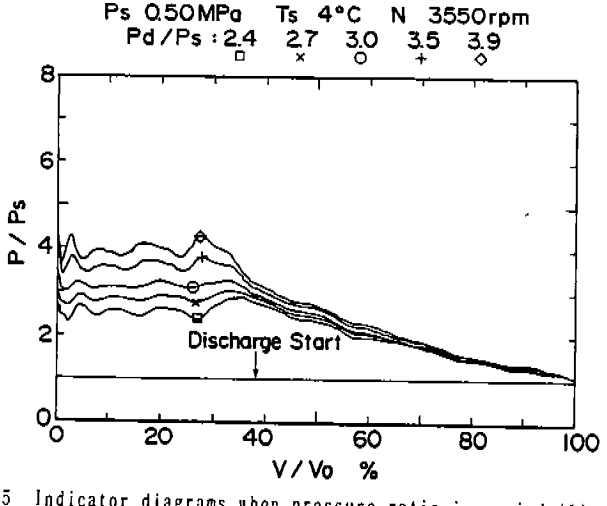

Fig. 5 Indicator diagrams when pressure ratio is varied (1)

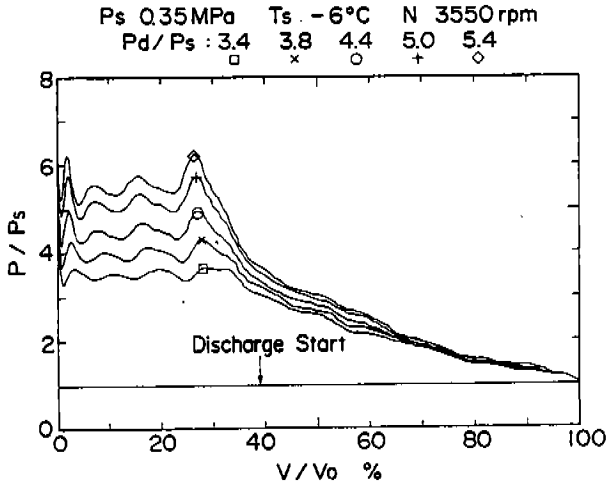

Fig. 6 Indicator diagrams when pressure ratio is varied (2)

5. Indicator diagram during changes in rotation speed

Fig. 7 shows volumetric efficiency ηv and adiabatic efficiency ηad when rotor rotation speed is varied while suction pressure is kept constant. The ratios shown are based on volumetric efficiency ηvo and adiabatic efficiency ηado at a rotation speed of 3500 rpm and discharge pressure of 1.53 MPa.

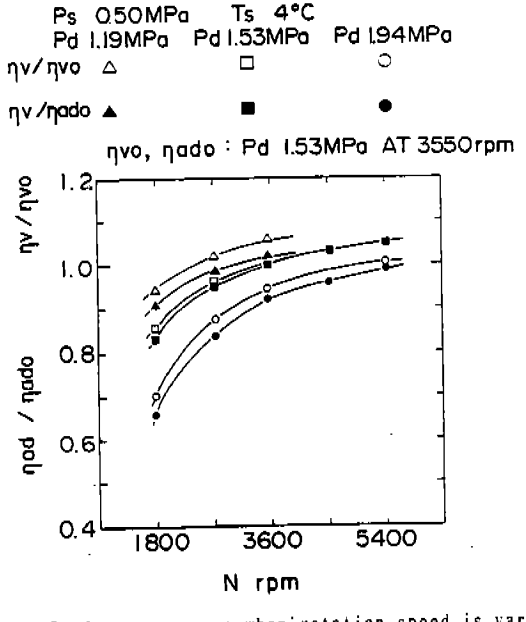

Fig. 7 Performance curve when rotation speed is varied

In the figure, the volumetric efficiency increases due to the increase of male rotor rotation speed, attributable to the fact that the increase in rotation speed results in the shortening of gas leakage time per groove.

Regarding changes in pressure ratio, the greater the pressure difference between the groove and the suction port, the greater the weight of leak gas. Therefore, the higher the discharge pressure, the lower the volumetric efficiency.

Regarding adiabatic efficiency, at Pd 1.53 MPa, which is close to the design pressure ratio of 3.0, the difference between volumetric efficiency and adiabatic efficiency is smaller than for other discharge pressures. This is due to the fact that under operating conditions which deviate from the design pressure ratio, the loss due to excessive compression increases inside the rotor groove, which is clear from the indicator diagrams obtained. Fig. 8 and Fig. 9 are indicator diagrams when rotation speed is varied while pressure ratio is kept constant. Looking at these figures, it can be seen that the gas pressure from the end of suction to the start of discharge is higher at lower rotation speeds and that there is much gas leakage from the upstream groove.

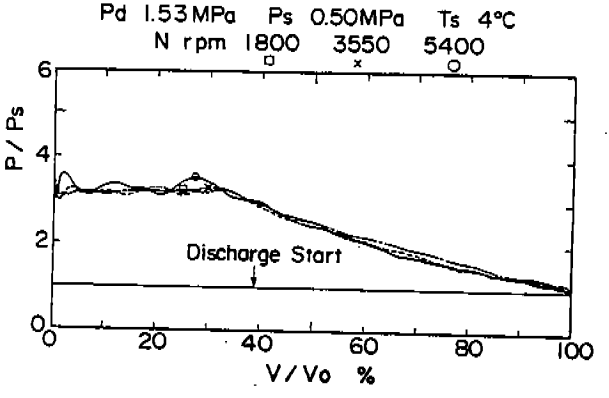

Fig. 8 Indicator diagrams when rotation speed is varied (1)

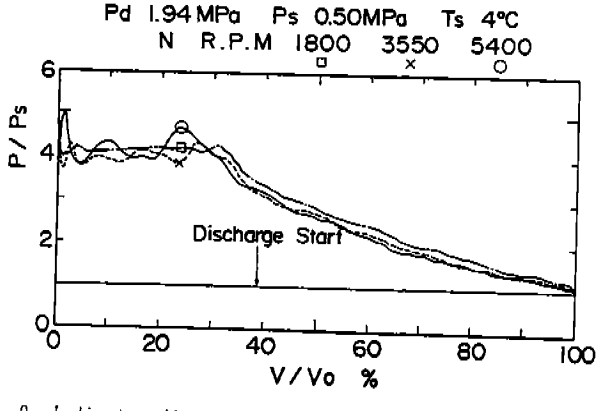

Fig. 9 Indicator diagrams when rotation speed is varied (2)

Once the discharge port is opened, as the discharge port area remains stable in relation to the change in rotation speed, and as the change of groove volume per time is large, gas inside the groove does not completely flow out, causing excessive compression, leading to power loss. For this reason, it is necessary to design the port for the high rotation speed range by taking into account the range of pressure increase during discharge.

Fig. 10 shows the pressure difference DP between the peak pressure value and the discharge port pressure value. This figure shows that the greater the rotation speed and the greater the deviation of pressure ratio from the built-in pressure ratio, the greater becomes the DP value during discharge, lowering adiabatic efficiency.

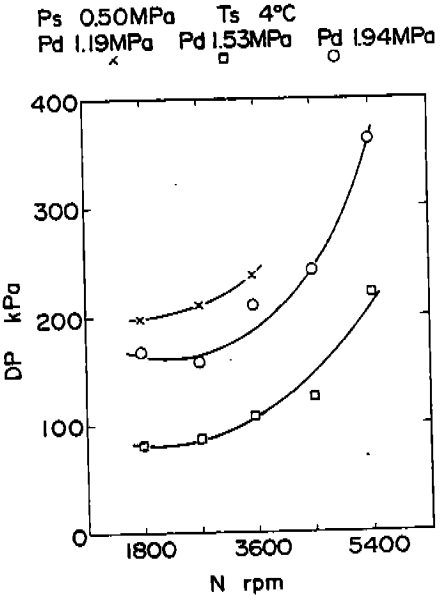

Fig. 10 Excessive compression inside groove

6. Comparison of indicated horsepower

Fig. 11 and Fig. 12 show the indicated horsepower and suction gas weight flow rate of the collected data in relation to the change in rotation speed while discharge pressure is varied in the range of 1.19 to 1.94 MPa but suction pressure is kept constant.

The indicator diagram varies greatly depending on pressure ratio and rotation speed. However, if correlated with the indicated horsepower and the suction gas weight flow rate, it is linear in relation to the change in rotation speed for each pressure ratio. Therefore, the reliability of the results of measurement and data processing could be confirmed.

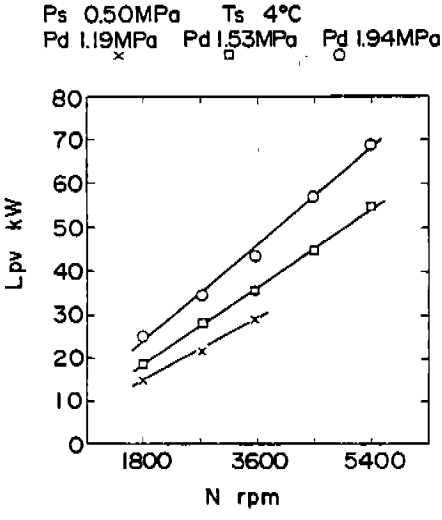

Fig. 11 Indicated horsepower when rotation speed is varied

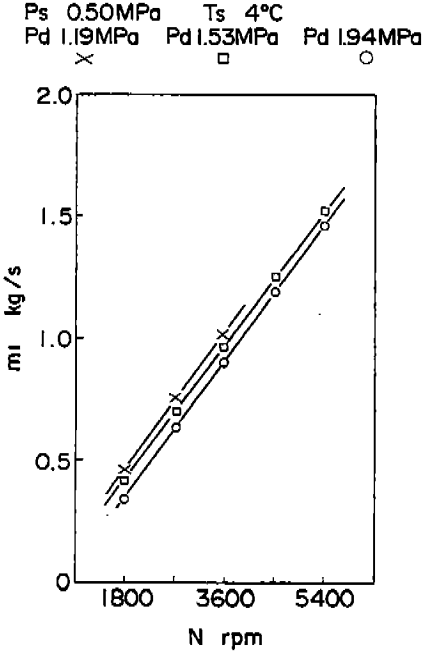

Fig. 12 Suction gas weight flow rate when rotation speed is varied

7. Conclusions

By plotting the indicator diagrams of a screw compressor, it was possible to grasp gas leakage conditions between grooves and changes in pressure on both sides of the port when rotation speed and pressure ratio were varied. By comparing the indicator diagrams thus collected, it was found that discharge pressure greatly affects the pressure in the rotor groove shortly before discharge.

Regarding operating conditions where both rotation speed and pressure ratio are above their respective design limits, for a high rotation speed it is necessary to design the port by taking into account the range of pressure increase at the time of discharge, but for a high pressure ratio, as there is no sudden pressure rise even shortly after the discharge port is opened, pressure ratio can be set in a wider range.

In the future, the author hopes to apply these measurement data to analyze seal gap flow conditions and pulsation phenomenon in the groove during discharge, from the standpoint of mixed phase (oil and gas) flow compression, aiming to improve simulation reliability.

This work is one of the R & D programs of Technology Research Association of Super Heat Pump Energy Accumulation System, entrusted by New Energy and Industrial Technology Development Organization (NEDO).

Reference:

(1) Singh, Pawan: J. Purdue Compressor Engineering Conf. (1984), 519
(2) Sangfors, B., Purdue Compressor Engineering Conf. (1984), 528